**Supporting Information**

# Rapid Antimicrobial Susceptibility Testing on Clinical Urine Samples by Video-based Object Scattering Intensity Detection

*Fenni Zhang[1,6], Jiapei Jiang[1,2], Michelle McBride[1], Xinyu Zhou[1,2], Yunze Yang[1], Manni Mo[1,3], Joseph Peterman[1], Thomas Grys*[4], Shelley E. Haydel*[1,5], Nongjian Tao[§1], and Shaopeng Wang*[1]*

1. Biodesign Center for Bioelectronics and Biosensors, Arizona State University, Tempe, AZ 85287, USA
2. School of Biological and Health Systems Engineering, Tempe, Arizona 85287, USA
3. School of Molecular Sciences, Arizona State University, Tempe, Arizona 85287, USA
4. Department of Laboratory Medicine and Pathology, Mayo Clinic, Phoenix, AZ 85054, USA
5. School of Life Sciences, Arizona State University, Tempe, Arizona 85287, USA
6. Biosensor National Special Laboratory, Key Laboratory for Biomedical Engineering of Education Ministry, Department of Biomedical Engineering, Zhejiang University, Hangzhou, 310027, PR China

*Corresponding authors:

Shaopeng Wang: shaopeng.wang@asu.edu

Shelley E. Haydel: shelley.haydel@asu.edu

Thomas E. Grys: Grys.Thomas@mayo.edu

§ Deceased in March 2020.

## S1. Background removal processing flow chart

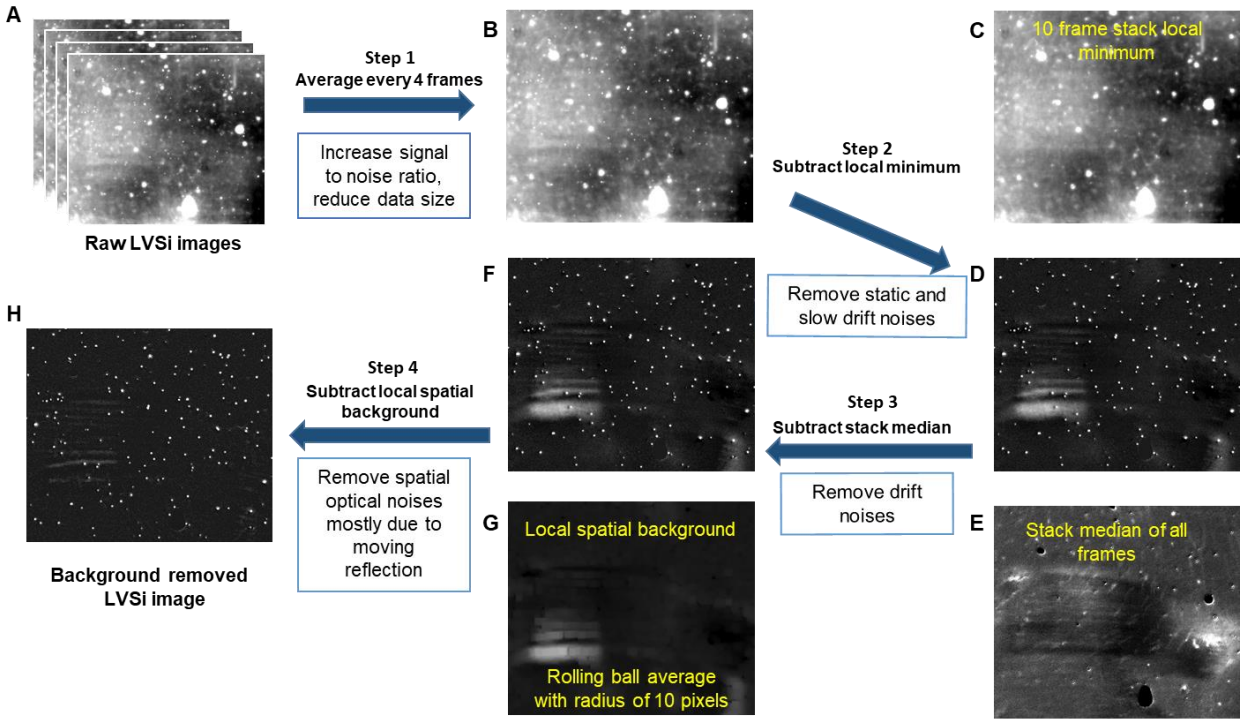


**Figure S1. Background removal processing flow chart. Step 1: Raw LVSi images recorded at 10 frames per second (A) are averaged for every 4 frames (B) to reduce noise and data size.** The size of the local stack average is set to avoid cell motion induced blur. **Step 2: Subtract stack local minimum (C) from (B) to remove static and slow drifting background noises (D).** Stack local minimum, the minimal intensity over a short time duration for each pixel, is calculated by minimum intensity projection of a small image stack. The stack size is set to be small to remove static and slow drift noises, while retaining bacteria that move beyond the original position in order to avoid loss of signal. **Step 3: Subtract stack median of all frames (E) from (D) to remove drift noises (F).** Stack median is calculated by median intensity projection of each pixel for the entire video stacks. **Step 4: Subtract local spatial background (G) from (F) to get the background free LVSi image (H).** Spatial local background of each pixel in the image is calculated by averaging over a large ball with radius of 10 pixels around the pixel to remove large spatial variations of the background intensities. The radius should be set to at least the size of the largest object that is not part of the background.

## S2. ROC curve for infection threshold determination

To determine the infection threshold, the results were evaluated using the receiver operating characteristic (ROC) curve constructed using $I_{Ct}/I_{C0}$ as a predictor. From the ROC curve for the first 20 samples, of which

10 were positive and 10 were negative from the clinical validation, we determined the infection threshold ($T_I$) of 1.1 with a sensitivity of 100% and a specificity of 100% at a 90 min testing time.

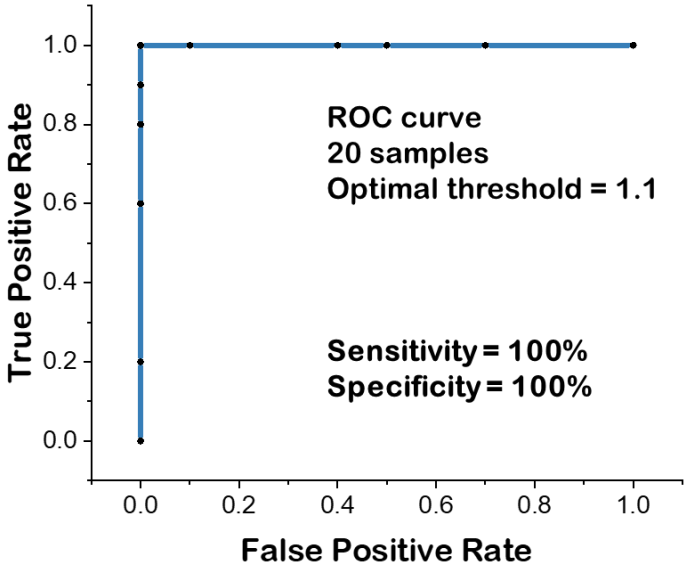


**Figure S2. ROC curve reveals 100% sensitivity and 100% specificity at 90 min with threshold of 1.1.**

**S3. OSID-AST with E. coli cultures at different concentrations**

To determine the dynamic range of OSID-AST method, we performed AST with *E. coli* cultures (concentrations ranging from $10^3$ to $10^7$ CFU/mL). The AST results and the corresponding raw intensity and the object intensity are plotted in Figure S3. At the low concentration of $10^3$ CFU/mL, both raw intensity and OSID analysis do not detect an obvious increase within 90 min. With longer testing times (170 min), the OSID analysis detects intensity increases, while raw intensity alone does not show obvious increases at the maximum time tested, 210 min. At concentrations between $10^4$ and $10^7$ CFU/mL, OSID method works well with the total AST time decreasing with increasing cell concentrations. Thus, the detection range of object intensity method is between $10^4$ and $10^7$ CFU/mL, while the raw intensity detection only accurately detects growth with concentrations above $10^6$ CFU/mL. In contrast, the single cell counting method needs lower concentrations, between $10^4$ and $10^5$ CFU/mL, to accurately enumerate increases in bacterial cells. Therefore, OSID-AST can accept a wider dynamic range of bacterial loads, which simplifies the sample preparation process while providing robust results.

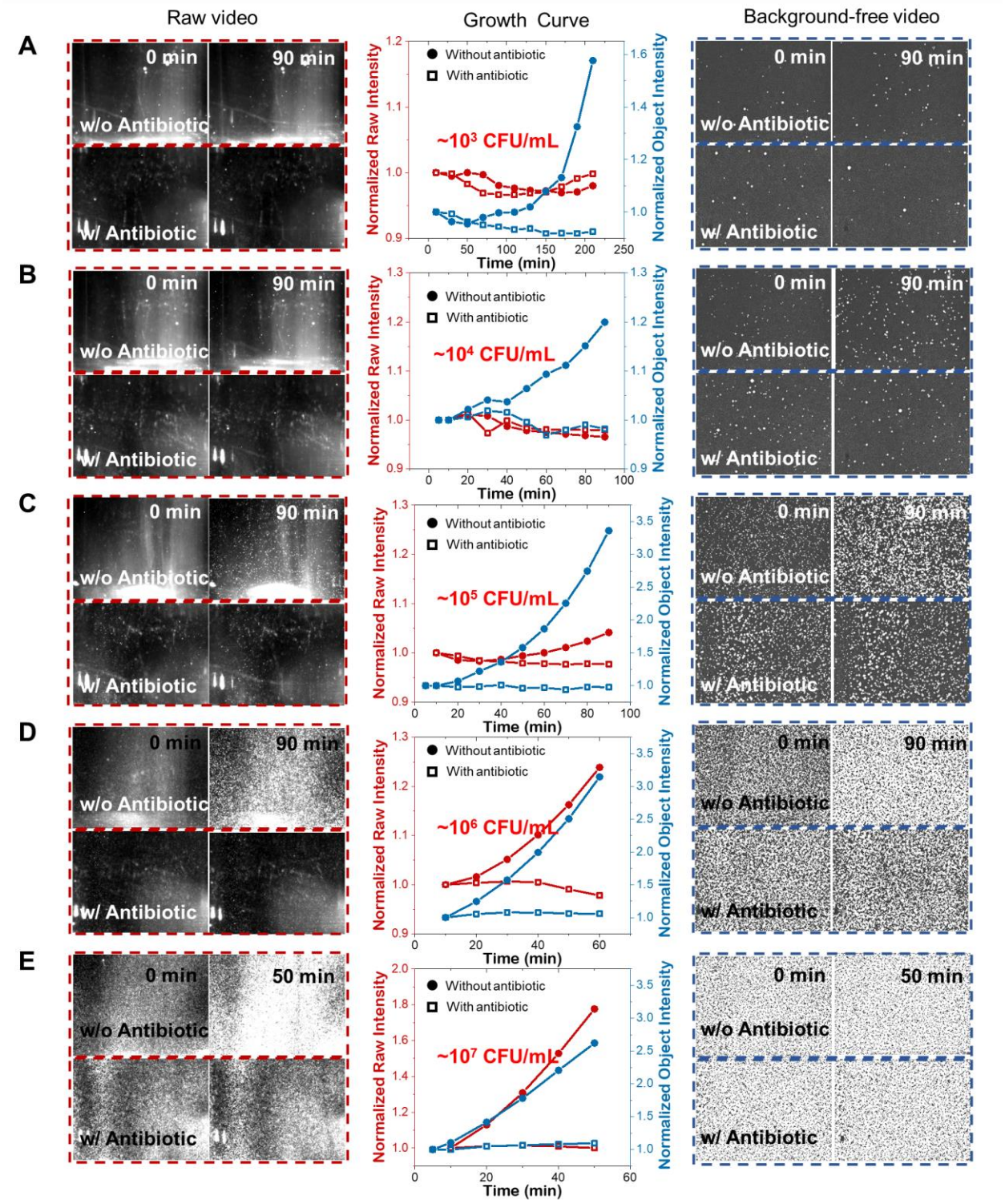


**Figure S3. OSID-AST with *E. coli* cultures of concentrations of $10^3$ (A), $10^4$ (B), $10^5$ (C), $10^6$ (D), $10^7$ (E) CFU/mL.**

**S4. Calibration curve between bacterial CFU concentrations and AST time**

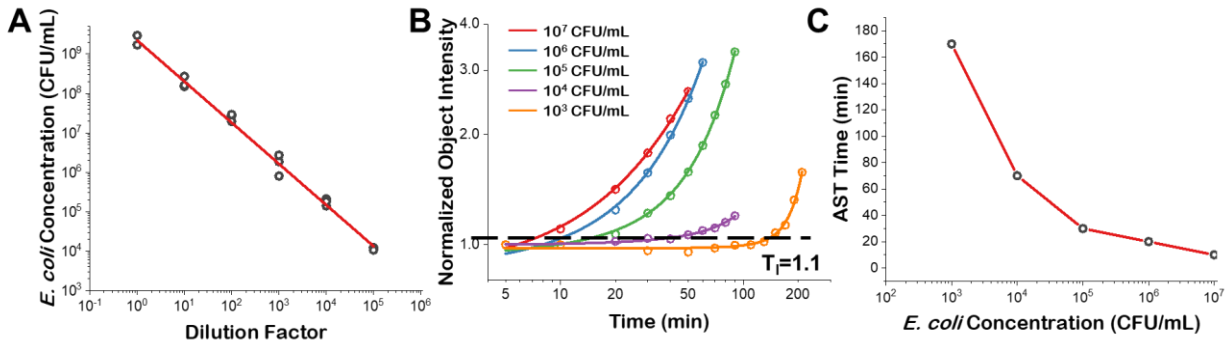


**Figure S4. Calibration between bacterial concentrations and AST time.** The plating validation of initial *E. coli* concentrations at different dilutions (A). *E. coli* growth curves with different initial cell concentrations ($10^3$-$10^7$ CFU/mL) (B). The calibration curve between bacterial concentration and AST time (C). The threshold for AST time determination is set at 1.1 as in panel B.

**S5. Comparison of object intensity detection and single cell counting for *E. coli* and *S. saprophyticus* cultures**

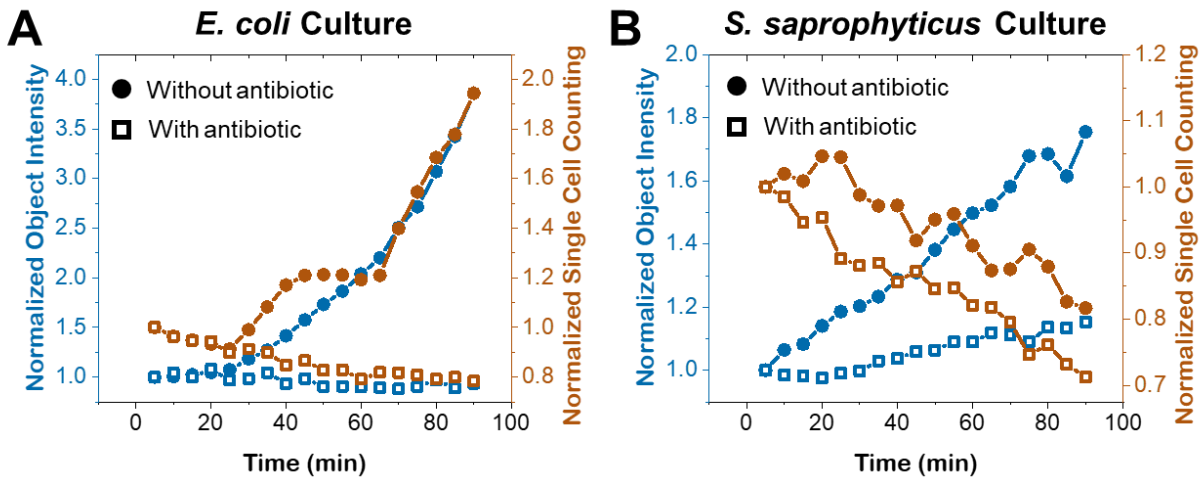


**Figure S5. Representative results of object intensity detection and single cell counting for pure *E. coli* (A) and *S. saprophyticus* (B) cultures.** Single cell counting accurately detected growth and susceptibility with *E. coli*, while object intensity accurately detected growth and susceptibility with both species.

**S6. Flow chart of the clinical sample preparation, testing and validation process**

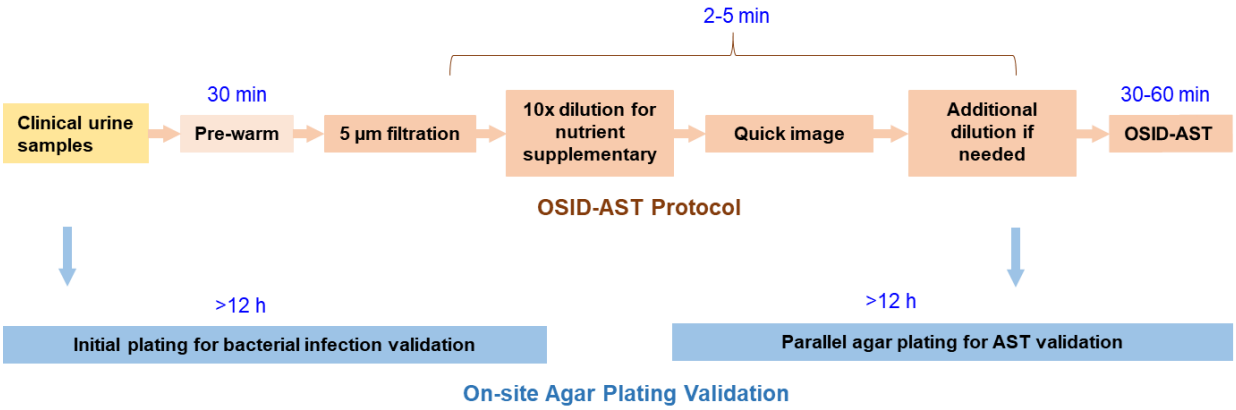


**Figure S6. Workflow of sample preparation, OSID-AST test and plating-based validations for clinical urine samples.**

## S7. Clinical urine sample ID results

**Table S1. OSID-AST detection ($I_{c90}/I_{c0}$) results of bacteriuria infection for 130 human patient samples compared with clinical results and on-site plating validation results**

| Sample # | Sample ID | Color | $I_{C90}/I_{C0}$ | OSID-AST Call | Clinical Lab Call* | Plating Validation Call# |
|---|---|---|---|---|---|---|
| 1 | ATU090319_01 | Yellow | 0.73776 | Negative† | Positive | Positive |
| 2 | ATU090319_02 | Yellow | 5.38214 | Positive | Positive | Positive |
| 4 | ATU090319_04 | Brown | 2.21285 | Positive | Positive | Positive |
| 6 | ATU090319_06 | Clear | 4.48616 | Positive | Positive | Positive |
| 8 | ATU090319_08 | Clear | 4.5611 | Positive | Positive | Positive |
| 10 | ATU090319_10 | Yellow | 3.1863 | Positive | Positive | Positive |
| 11 | ATU091019_01 | Yellow | 1.16772 | Positive | Positive | Positive |
| 13 | ATU091019_03 | Yellow | 5.20085 | Positive | Positive | Positive |
| 15 | ATU091019_05 | Milky | 0.8132 | Negative† | Positive | Positive |
| 17 | ATU091019_07 | Milky | 2.04085 | Positive | Positive | Positive |
| 18 | ATU091019_08 | Cloudy | 4.8725 | Positive | Positive | Positive |
| 21 | ATU092419_01 | Milky | 6.48988 | Positive | Positive | Positive |
| 22 | ATU092419_02 | Milky | 7.17449 | Positive | Positive | Positive |
| 26 | ATU092419_06 | Milky | 2.53505 | Positive | Positive | Positive |
| 27 | ATU092419_07 | Yellow | 0.80355 | Negative† | Positive | Positive |
| 28 | ATU092419_08 | Milky | 0.63273 | Negative† | Positive | Positive |
| 31 | ATU100119_01 | Milky | 4.073 | Positive | Positive | Positive |
| 33 | ATU100119_03 | Clear | 3.6801 | Positive | Positive | Positive |
| 35 | ATU100119_05 | Clear | 5.3097 | Positive | Positive | Positive |
| 36 | ATU100119_06 | Cloudy | 6.70157 | Positive | Positive | Positive |
| 38 | ATU100119_08 | Cloudy | 0.72527 | Negative† | Positive | Positive |
| 44 | ATU100819_04 | Milky | 7.42181 | Positive | Positive | Positive |
| 45 | ATU100819_05 | Milky | 7.68108 | Positive | Positive | Positive |
| 46 | ATU100819_06 | Milky | 4.12703 | Positive | Positive | Positive |
| 49 | ATU100819_09 | Milky | 5.10955 | Positive | Positive | Positive |
| 50 | ATU100819_10 | Milky | 0.75666 | Negative† | Positive | Positive |
| 51 | ATU101519_01 | Yellow | 0.89931 | Negative† | Positive | Negative† |
| 52 | ATU101519_02 | Milky | 4.23241 | Positive | Positive | Positive |
| 53 | ATU101519_03 | Clear | 5.32849 | Positive | Positive | Positive |
| 57 | ATU101519_07 | Milky | 5.19027 | Positive | Positive | Positive |
| 58 | ATU101519_08 | Milky | 6.19954 | Positive | Positive | Positive |
| 61 | ATU102219_01 | Yellow | 5.12761 | Positive | Positive | Positive |
| 62 | ATU102219_02 | Clear | 8.17162 | Positive | Positive | Positive |
| 63 | ATU102219_03 | Clear | 2.50728 | Positive | Positive | Positive |
| 64 | ATU102219_04 | Clear | 7.79974 | Positive | Positive | Positive |
| 69 | ATU102219_09 | Milky | 5.60933 | Positive | Positive | Positive |
| 71 | ATU102919_01 | Milky | 1.96968 | Positive | Positive | Positive |
| 72 | ATU102919_02 | Yellow | 1.13846 | Positive | Positive | Positive |
| 73 | ATU102919_03 | Yellow | 5.47704 | Positive | Positive | Positive |
| 79 | ATU102919_09 | Milky | 6.25799 | Positive | Positive | Positive |
| 80 | ATU102919_10 | Milky | 2.46932 | Positive | Positive | Positive |
| 83 | ATU111219_03 | Cloudy | 2.51224 | Positive | Positive | Positive |
| 84 | ATU111219_04 | Yellow | 6.27751 | Positive | Positive | Positive |
| 85 | ATU111219_05 | Milky | 0.88083 | Negative† | Positive | Positive |
| 89 | ATU111219_09 | Cloudy | 0.72358 | Negative† | Positive | Positive |
| 90 | ATU111219_10 | Yellow | 4.27291 | Positive | Positive | Positive |
| 93 | ATU120319_03 | Milky | 4.75435 | Positive | Positive | Positive |
| 96 | ATU120319_06 | Milky | 4.74752 | Positive | Positive | Positive |
| 97 | ATU120319_07 | Clear | 1.44209 | Positive | Positive | Positive |
| 99 | ATU120319_09 | Milky | 1.22829 | Positive | Positive | Positive |
| 100 | ATU120319_10 | Yellow | 2.89034 | Positive | Positive | Positive |
| 102 | ATU121019_02 | Clear | 6.36563 | Positive | Positive | Positive |
| 104 | ATU121019_04 | Clear | 0.87916 | Negative† | Positive | Positive |
| 106 | ATU121019_06 | Cloudy | 3.58189 | Positive | Positive | Positive |
| 108 | ATU121019_08 | Cloudy | 1.6952 | Positive | Positive | Positive |
| 110 | ATU121019_10 | Milky | 2.72788 | Positive | Positive | Positive |
| 113 | ATU010720_03 | Milky | 2.03288 | Positive | Positive | Positive |
| 114 | ATU010720_04 | Milky | 3.19438 | Positive | Positive | Positive |
| 116 | ATU010720_06 | Milky | 2.32701 | Positive | Positive | Positive |
| 117 | ATU010720_07 | Cloudy | 1.97967 | Positive | Positive | Positive |
| 118 | ATU010720_08 | Cloudy | 5.8613 | Positive | Positive | Positive |
| 124 | ATU011420_04 | Milky | 5.88689 | Positive | Positive | Positive |
| 125 | ATU011420_05 | Milky | 0.96676 | Negative† | Positive | Negative† |
| 128 | ATU011420_08 | Clear | 2.38955 | Positive | Positive | Positive |
| 129 | ATU011420_09 | Cloudy | 5.39929 | Positive | Positive | Positive |
| 130 | ATU011420_10 | Milky | 1.24704 | Positive | Positive | Positive |

| | | | | | | |
|---|---|---|---|---|---|---|
| 3 | ATU090319_03 | Clear | 0.46777 | Negative | Negative | Negative |
| 5 | ATU090319_05 | Clear | 0.6696 | Negative | Negative | Negative |
| 7 | ATU090319_07 | Clear | 0.81648 | Negative | Negative | Negative |
| 9 | ATU090319_09 | Clear | 0.76041 | Negative | Negative | Negative |
| 12 | ATU091019_02 | Yellow | 0.86645 | Negative | Negative | Negative |
| 14 | ATU091019_04 | Yellow | 0.93563 | Negative | Negative | Negative |
| 16 | ATU091019_06 | Clear | 0.80403 | Negative | Negative | Negative |
| 19 | ATU091019_09 | Clear | 0.90393 | Negative | Negative | Negative |
| 20 | ATU091019_10 | Clear | 0.88178 | Negative | Negative | Negative |
| 23 | ATU092419_03 | Cloudy | 0.77362 | Negative | Negative | Negative |
| 24 | ATU092419_04 | Clear | 0.57816 | Negative | Negative | Negative |
| 25 | ATU092419_05 | Clear | 0.78313 | Negative | Negative | Negative |
| 29 | ATU092419_09 | Clear | 0.79639 | Negative | Negative | Negative |
| 30 | ATU092419_10 | Cloudy | 0.78 | Negative | Negative | Negative |
| 32 | ATU100119_02 | Clear | 0.98838 | Negative | Negative | Negative |
| 34 | ATU100119_04 | Clear | 0.69371 | Negative | Negative | Negative |
| 37 | ATU100119_07 | Clear | 0.90024 | Negative | Negative | Negative |
| 39 | ATU100119_09 | Milky | 0.84636 | Negative | Negative | Negative |
| 40 | ATU100119_10 | Clear | 0.86164 | Negative | Negative | Negative |
| 41 | ATU100819_01 | Yellow | 0.56269 | Negative | Negative | Negative |
| 42 | ATU100819_02 | Clear | 0.83746 | Negative | Negative | Negative |
| 43 | ATU100819_03 | Yellow | 0.87212 | Negative | Negative | Negative |
| 47 | ATU100819_07 | Clear | 0.87622 | Negative | Negative | Negative |
| 48 | ATU100819_08 | Clear | 0.90836 | Negative | Negative | Negative |
| 54 | ATU101519_04 | Clear | 0.90369 | Negative | Negative | Negative |
| 55 | ATU101519_05 | Milky | 0.61539 | Negative | Negative | Negative |
| 56 | ATU101519_06 | Cloudy | 0.1912 | Negative | Negative | Negative |
| 59 | ATU101519_09 | Cloudy | 0.48572 | Negative | Negative | Negative |
| 60 | ATU101519_10 | Cloudy | 0.49874 | Negative | Negative | Negative |
| 65 | ATU102219_05 | Yellow | 0.41149 | Negative | Negative | Negative |
| 66 | ATU102219_06 | Yellow | 0.6527 | Negative | Negative | Negative |
| 67 | ATU102219_07 | Clear | 0.82163 | Negative | Negative | Negative |
| 68 | ATU102219_08 | Clear | 0.67353 | Negative | Negative | Negative |
| 70 | ATU102219_10 | Clear | 0.5757 | Negative | Negative | Negative |
| 74 | ATU102919_04 | Yellow | 0.85456 | Negative | Negative | Negative |
| 75 | ATU102919_05 | Milky | 0.33682 | Negative | Negative | Negative |
| 76 | ATU102919_06 | Yellow | 0.83996 | Negative | Negative | Negative |
| 77 | ATU102919_07 | Clear | 0.8318 | Negative | Negative | Negative |
| 78 | ATU102919_08 | Clear | 0.91851 | Negative | Negative | Negative |
| 81 | ATU111219_01 | Yellow | 0.85783 | Negative | Negative | Negative |
| 82 | ATU111219_02 | Yellow | 0.9487 | Negative | Negative | Negative |
| 86 | ATU111219_06 | Clear | 0.8654 | Negative | Negative | Negative |
| 87 | ATU111219_07 | Yellow | 0.44171 | Negative | Negative | Negative |
| 88 | ATU111219_08 | Yellow | 0.89734 | Negative | Negative | Negative |
| 91 | ATU120319_01 | Milky | 0.91473 | Negative | Negative | Negative |
| 92 | ATU120319_02 | Yellow | 0.68496 | Negative | Negative | Negative |
| 94 | ATU120319_04 | Yellow | 0.82697 | Negative | Negative | Negative |
| 95 | ATU120319_05 | Yellow | 0.90686 | Negative | Negative | Negative |
| 98 | ATU120319_08 | Clear | 0.8935 | Negative | Negative | Negative |
| 101 | ATU121019_01 | Milky | 0.97041 | Negative | Negative | Negative |
| 103 | ATU121019_03 | Yellow | 0.90842 | Negative | Negative | Negative |
| 105 | ATU121019_05 | Clear | 0.93901 | Negative | Negative | Negative |
| 107 | ATU121019_07 | Clear | 0.97536 | Negative | Negative | Negative |
| 109 | ATU121019_09 | Yellow | 0.88897 | Negative | Negative | Negative |
| 111 | ATU010720_01 | Clear | 0.92131 | Negative | Negative | Negative |
| 112 | ATU010720_02 | Clear | 0.94069 | Negative | Negative | Negative |
| 115 | ATU010720_05 | Clear | 0.95538 | Negative | Negative | Negative |
| 119 | ATU010720_09 | Clear | 0.90791 | Negative | Negative | Negative |
| 120 | ATU010720_10 | Yellow | 0.9299 | Negative | Negative | Negative |
| 121 | ATU011420_01 | Yellow | 0.91915 | Negative | Negative | Negative |
| 122 | ATU011420_02 | Clear | 0.92376 | Negative | Negative | Negative |
| 123 | ATU011420_03 | Cloudy | 0.76016 | Negative | Negative | Negative |
| 126 | ATU011420_06 | Clear | 0.95965 | Negative | Negative | Negative |
| 127 | ATU011420_07 | Yellow | 0.94512 | Negative | Negative | Negative |

***** Reference method (Traditional plating followed by BD Phoenix™ automated AST) results generated by the Mayo Clinic microbiology lab.

[#] On-site validation results generated by overnight plating upon sample receiving.

[†] Disagreement between OSID-AST and reference method results.

**S8. Initial sample validation results**

On-site initial bacterial load validation is performed with sample plating and colony counting. Upon urine sample reception, samples were subjected to serial dilutions and plated on LB agar for colony enumeration. This plating validation provides initial bacterial concentration references and reveals any viability changes during sample storage and transportation. While 66 of 130 clinical samples were confirmed to have greater than $10^3$ CFU per mL, two of these contained concentrations below the clinical threshold of $10^4$ CFU/mL, and six had bacterial concentrations that were 10-100 times less than those initially determined by Mayo Clinic (Figure S7), before storage and transport. Therefore, we anticipate greater accuracy when rapid AST is performed in POC settings and this loss in bacterial viability is avoided.

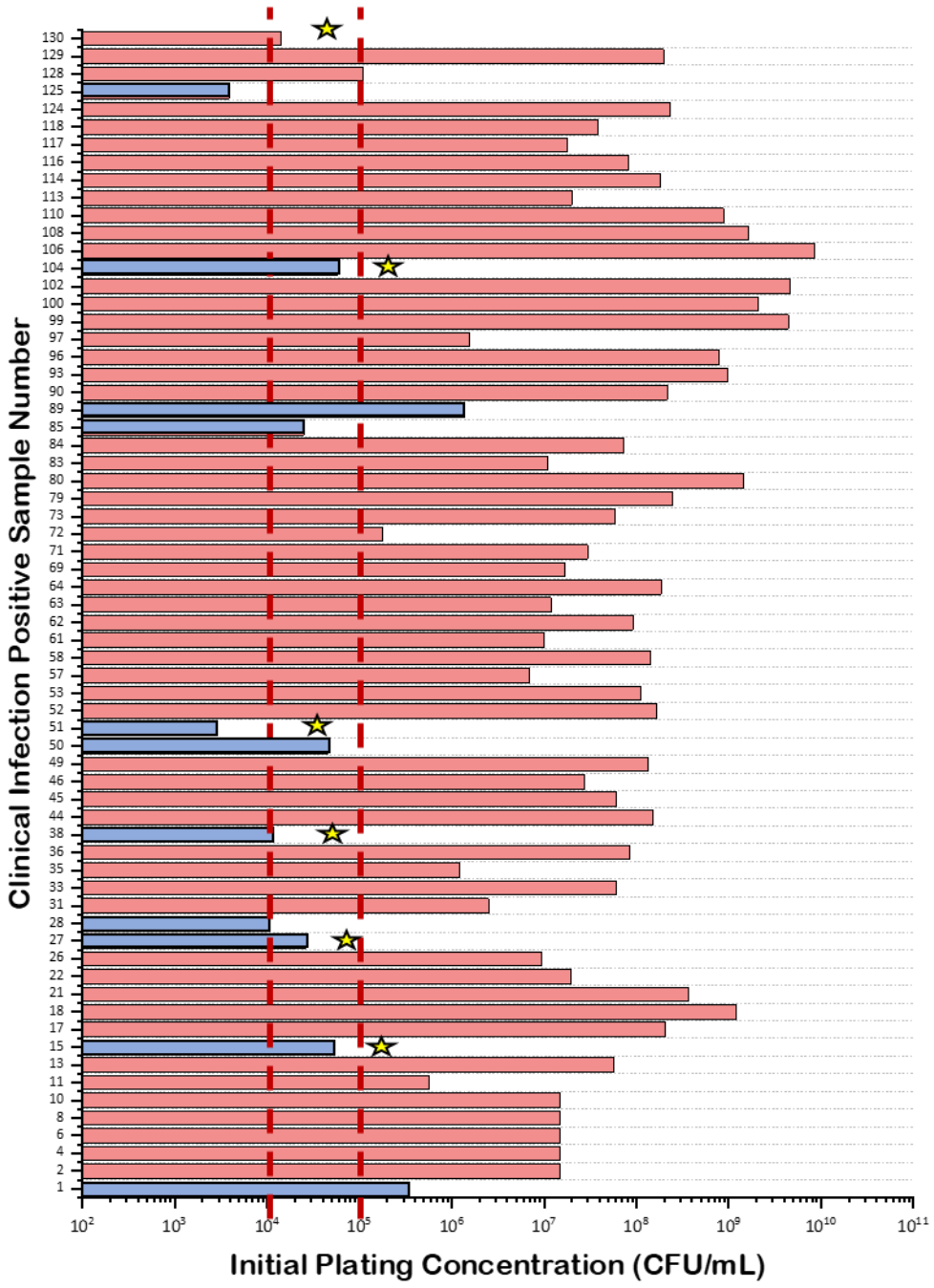


**Figure S7. Initial plating validation of all 66 clinically determined positive sample. The blue bar shows the initial bacterial concentration of 11 false negative samples.** The red dashed lines indicate the clinical infection threshold ($10^4$-$10^5$ CFU/mL). The stars indicate the urine samples with initial plating concentrations less than those determined by Mayo Clinic (prior to storage and transport).

**S9. Initial and parallel plating validation result of 11 false negative samples**

Parallel plating validation was performed along with LVSi detection to test the samples post-preparation. Initial plating CFU/mL determinations, calculated CFU/mL based on sample dilution, and parallel plating of sample post-preparation of 11 false negatives samples are presented here. The parallel plating validation results show low counts of bacterial cells (below 1000 cells/mL), after all sample handling, including prewarming, filtration and dilution. Dilutions of these samples ranged from 10 to 1000 times such that both single cell counting and object scattering intensity could be performed. Since the OSID-AST method functions at a higher particle concentration range ($10^4$ to $10^7$ CFU/mL), we estimate that 7 out of 11 of these false negative results could be avoided with an optimized dilution scheme and quicker handling process at the POC settings.

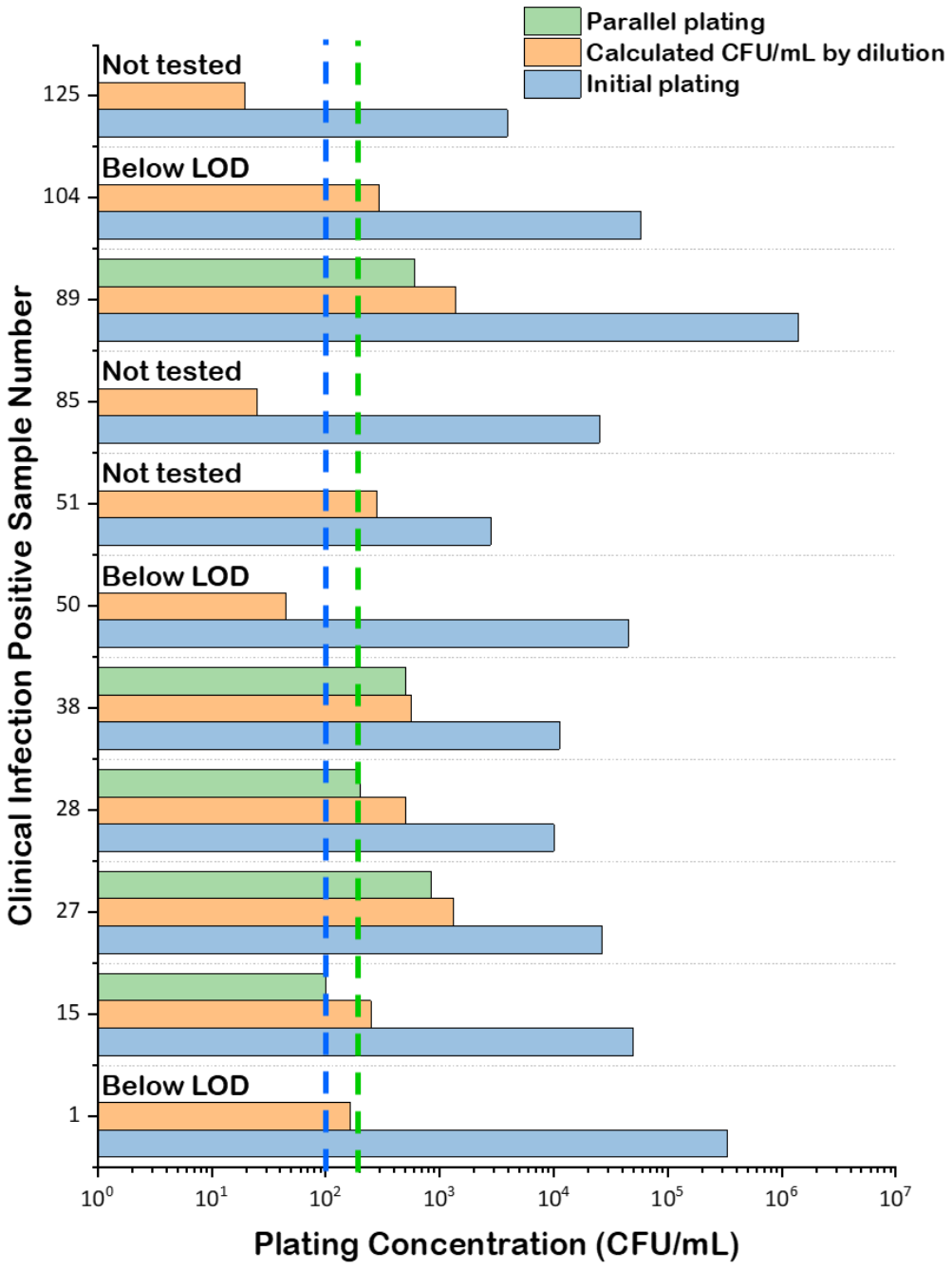


**Figure S8. The comparison of initial plating, calculated CFU/mL by dilution, and the parallel plating results of 11 false negatives samples.** The plating results are the mean value of three replicates. The limit of detection (LOD, blue hatched line) for initial plating (blue bar) is 100 CFU/mL. The limit of detection (LOD, green hatched line) for parallel plating (green bar) is 200 CFU/mL. When parallel plating was performed but colonies were not detected in all three replicates (sample #1, #51, #105), the samples are marked as 'Below LOD'.

**S10. Examples of false negative samples by single cell counting, positive by OSID**

Each sample was analyzed with both the single cell counting method and the OSID method. Two examples are presented here. The single cell counting detection, which needs extra manual cell detection and tracking processing, showed 17 false negative samples out of 130 tested samples, a 6 sample increase compared to the object intensity detection method. The OSID method measures both cell growth and elongation, while cell counting alone tracks the sum of distinct individual particles and thus detects an increase only after elongated cells divide and daughter cells separate.

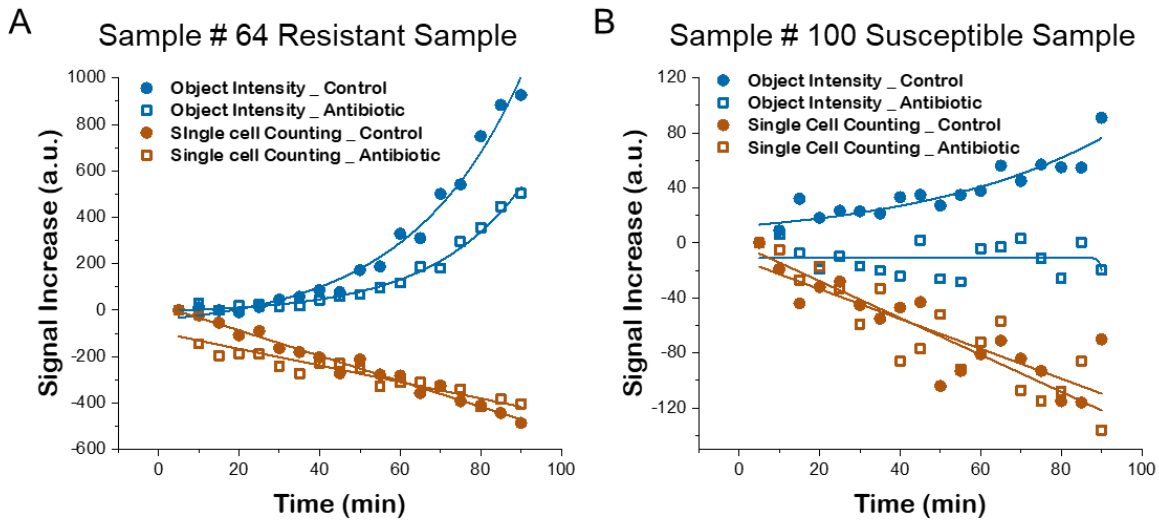


**Figure S9. Two examples of false negative results as determined by single cell counting, which were correctly identified as positive for infection by object intensity detection.** Example of an infection positive sample that is resistant to ciprofloxacin (2 μg/mL) (A). Example of an infection positive sample that is susceptible to ciprofloxacin (2 μg/mL) (B).

**S11. Clinical urine sample AST results**

**Table 2. OSID-AST of 55 bacteriuria-positive human urine samples compared to clinical and onsite plating validation results**

| Sample # | Sample ID | Comments | $\Delta I_{ABX}/\Delta I_C$ | OSID-AST Call | Clinical Lab Call* | Plating Validation Call# |
|---|---|---|---|---|---|---|
| 1 | ATU090319_01 | 2 Isolates: >100,000 cfu/mL KLEBSIELLA PNEUMONIAE ; 10,000-100,000 cfu/mL ENTEROCOCCUS FAECALIS | N/A | Negative† | S | S |
| 2 | ATU090319_02 | >100,000 cfu/mL ESCHERICHIA COLI | 0.94068 | R | R | R |
| 4 | ATU090319_04 | >100,000 cfu/mL ESCHERICHIA COLI | 0.03015 | S | S | NT |
| 6 | ATU090319_06 | >100,000 cfu/mL ESCHERICHIA COLI | 1.26833 | R | R | R |
| 8 | ATU090319_08 | >100,000 cfu/mL ESCHERICHIA COLI | -0.05981 | S | S | NT |
| 10 | ATU090319_10 | >100,000 cfu/mL KLEBSIELLA AEROGENES | 0.24834 | S | S | S |
| 11 | ATU091019_01 | >100,000 cfu/mL ESCHERICHIA COLI | -0.35376 | S | S | NT |
| 13 | ATU091019_03 | >100,000 cfu/mL ESCHERICHIA COLI | 0.01426 | S | S | S |
| 15 | ATU091019_05 | >100,000 cfu/mL ESCHERICHIA COLI | N/A | Negative† | S | S |
| 17 | ATU091019_07 | >100,000 cfu/mL GRAM NEGATIVE BACILLUS | 1.76005 | R | R | R |
| 18 | ATU091019_08 | >100,000 cfu/mL GRAM NEGATIVE BACILLUS | 0.56815 | R | R | R |
| 21 | ATU092419_01 | >100,000 cfu/mL ESCHERICHIA COLI | 0.01376 | S | S | NT |
| 22 | ATU092419_02 | >100,000 cfu/mL ESCHERICHIA COLI | 0.1729 | S | S | NT |
| 26 | ATU092419_06 | >100,000 cfu/mL ENTEROBACTER CLOACAE | 0.01948 | S | S | S |
| 27 | ATU092419_07 | >100,000 cfu/mL GRAM NEGATIVE BACILLUS | N/A | Negative† | S | S |
| 28 | ATU092419_08 | 10,000-100,000 cfu/mL GRAM NEGATIVE BACILLUS | N/A | Negative† | R | R |
| 31 | ATU100119_01 | >100,000 cfu/mL ESCHERICHIA COLI | 2.30E-04 | S | S | NT |
| 33 | ATU100119_03 | >100,000 cfu/mL ESCHERICHIA COLI | -0.09991 | S | S | NT |
| 35 | ATU100119_05 | >100,000 cfu/mL ESCHERICHIA COLI | 0.95614 | R | R | NT |
| 36 | ATU100119_06 | >100,000 cfu/mL ESCHERICHIA COLI | 0.04334 | S | S | S |
| 38 | ATU100119_08 | >100,000 cfu/mL GRAM NEGATIVE BACILLUS | N/A | Negative† | S | S |
| 44 | ATU100819_04 | >100,000 cfu/mL ESCHERICHIA COLI | 0.98483 | R | R | NT |
| 45 | ATU100819_05 | >100,000 cfu/mL ESCHERICHIA COLI | 0.0119 | S | S | NT |
| 46 | ATU100819_06 | >100,000 cfu/mL ESCHERICHIA COLI | 1.19128 | R | R | R |
| 49 | ATU100819_09 | >100,000 cfu/mL ESCHERICHIA COLI | 0.02571 | S | S | S |
| 50 | ATU100819_10 | 10,000-100,000 cfu/mL ESCHERICHIA COLI | N/A | Negative† | S | S |
| 51 | ATU101519_01 | >100,000 cfu/mL ESCHERICHIA COLI | N/A | Negative† | S | NT |
| 52 | ATU101519_02 | >100,000 cfu/mL ESCHERICHIA COLI | -0.00858 | S | S | NT |
| 53 | ATU101519_03 | >100,000 cfu/mL KLEBSIELLA PNEUMONIAE | 0.20227 | S | S | NT |
| 57 | ATU101519_07 | >100,000 cfu/mL ESCHERICHIA COLI | 0.14571 | S | S | S |
| 58 | ATU101519_08 | >100,000 cfu/mL GRAM NEGATIVE BACILLUS | 0.30196 | S | S | S |
| 61 | ATU102219_01 | >100,000 cfu/mL ESCHERICHIA COLI | -0.07596 | S | S | NT |
| 62 | ATU102219_02 | >100,000 cfu/mL ESCHERICHIA COLI | 0.85396 | R | R | NT |
| 63 | ATU102219_03 | >100,000 cfu/mL ESCHERICHIA COLI | 0.8574 | R | R | NT |
| 64 | ATU102219_04 | >100,000 cfu/mL KLEBSIELLA PNEUMONIAE | 0.1025 | S | S | NT |
| 69 | ATU102219_09 | >100,000 cfu/mL KLEBSIELLA sp | 0.4051 | S | S | S |
| 71 | ATU102919_01 | >100,000 cfu/mL ESCHERICHIA COLI | -0.03695 | S | S | NT |
| 72 | ATU102919_02 | >100,000 cfu/mL ESCHERICHIA COLI | -1.14431 | S | S | S |
| 73 | ATU102919_03 | >100,000 cfu/mL ESCHERICHIA COLI | 0.07311 | S | S | S |
| 79 | ATU102919_09 | >100,000 cfu/mL ESCHERICHIA COLI | 0.09926 | S | S | S |
| 80 | ATU102919_10 | >100,000 cfu/mL CITROBACTER FREUNDII COMPLEX | 1.14637 | R[a] | S | S |
| 83 | ATU111219_03 | >100,000 cfu/mL ESCHERICHIA COLI | -0.06239 | S | S | NT |
| 84 | ATU111219_04 | >100,000 cfu/mL KLEBSIELLA PNEUMONIAE | 0.13194 | S | S | NT |
| 85 | ATU111219_05 | 10,000-100,000 cfu/mL KLEBSIELLA PNEUMONIAE | N/A | Negative† | R | NT |
| 89 | ATU111219_09 | >100,000 cfu/mL PSEUDOMONAS AERUGINOSA | N/A | Negative† | N/A | S |
| 90 | ATU111219_10 | >100,000 cfu/mL ENTEROBACTER CLOACAE | 0.2266 | S | N/A | S |
| 93 | ATU120319_03 | >100,000 cfu/mL ESCHERICHIA COLI | 0.22734 | S | S | S |
| 96 | ATU120319_06 | >100,000 cfu/mL ESCHERICHIA COLI | 1.12652 | R | R | NT |
| 97 | ATU120319_07 | 10,000-100,000 cfu/mL ESCHERICHIA COLI | 1.45551 | R | R | NT |
| 99 | ATU120319_09 | >100,000 cfu/mL ESCHERICHIA COLI | -0.07618 | S | S | NT |
| 100 | ATU120319_10 | >100,000 cfu/mL KLEBSIELLA PNEUMONIAE | 0.10105 | S | S | NT |
| 102 | ATU121019_02 | >100,000 cfu/mL ESCHERICHIA COLI | 0.40565 | S | S | S |
| 104 | ATU121019_04 | >100,000 cfu/mL ESCHERICHIA COLI | N/A | Negative† | S | S |
| 106 | ATU121019_06 | >100,000 cfu/mL ESCHERICHIA COLI | 0.87237 | R | R | NT |
| 108 | ATU121019_08 | >100,000 cfu/mL ESCHERICHIA COLI | 0.27158 | S | S | NT |
| 110 | ATU121019_10 | >100,000 cfu/mL KLEBSIELLA PNEUMONIAE | 0.4057 | S | S | NT |
| 113 | ATU010720_03 | >100,000 cfu/mL ESCHERICHIA COLI | 0.03975 | S | S | NT |
| 114 | ATU010720_04 | >100,000 cfu/mL ESCHERICHIA COLI | -0.00101 | S | S | NT |
| 116 | ATU010720_06 | >100,000 cfu/mL ESCHERICHIA COLI | 0.01551 | S | S | S |
| 117 | ATU010720_07 | >100,000 cfu/mL ESCHERICHIA COLI | 0.95502 | R | R | R |
| 118 | ATU010720_08 | >100,000 cfu/mL KLEBSIELLA PNEUMONIAE | 0.16467 | S | S | S |
| 124 | ATU011420_04 | >100,000 cfu/mL ESCHERICHIA COLI | 1.03449 | R | R | NT |
| 125 | ATU011420_05 | 10,000-100,000 cfu/mL ESCHERICHIA COLI | N/A | Negative† | S | NT |
| 128 | ATU011420_08 | 10,000-100,000 cfu/mL ESCHERICHIA COLI | -0.16487 | S | S | S |
| 129 | ATU011420_09 | >100,000 cfu/mL ESCHERICHIA COLI | 1.29926 | R | R | R |
| 130 | ATU011420_10 | >100,000 cfu/mL ESCHERICHIA COLI | 0.91598 | R | R | R |

***** Reference method (Traditional plating followed by BD Phoenix™ automated AST) results generated by the Mayo Clinic microbiology lab.

**#** On-site validation results generated by overnight plating upon sample receiving.

† False negative results by OSID-AST.

[a] Mis-categorization occurred if reference method indicated susceptible and OSID-AST indicated resistant.

## S12. Clinical Sample # 80

For AST of 55 positive samples, one susceptible sample was mis-categorized as resistant by OSID-AST (Sample # 80, Supporting Information S11, Table S2), which contains >100,000 CFU/mL *Citrobacter freundii* Complex. To elucidate this inconsistency, a validation experiment was performed. Since the original clinical sample was no longer available, we used cryogenically-preserved clinical sample # 80 for this validation experiment. Briefly, frozen cells were inoculated onto LB agar and incubated overnight (~ 15 h) at 37 ℃. Then, bacteria were spiked into pooled urine (BioIVT Human Urine Pooled Gender) with a concentration of ~ $10^9$ CFU/mL and stored at 4 ℃ overnight to simulate clinical sample conditions. For LVSi imaging, the spiked urine sample were processed as the flowchart in Figure S6 for OSID-AST detection, and high magnification microscopy (80×) images were recorded during AST detection for morphology validation.

LVSi video and high magnification images (80× microscopic imaging) of the cultured isolates from the sample were shown in Figure S10, and obvious elongation of the bacteria under 2 μg/mL ciprofloxacin were detected, which induced object intensity increase in OSID-AST system similar to the control (antibiotic free) sample within the 90 min measurement time (Figure S10 A & B). With longer measurement times, the normalized growth curve with 2 μg/mL ciprofloxacin (Figure S10 C & D) plateaued around 2 h after the intensity roughly doubled, which means the cells stopped growing after reaching maximum length, as the antibiotics prevented DNA replication and cell division. In contrast, the cells without antibiotics grew exponentially. Therefore, for this elongation case, longer detection time is needed for accurate OSID-AST detection (Figure S10 C & D).

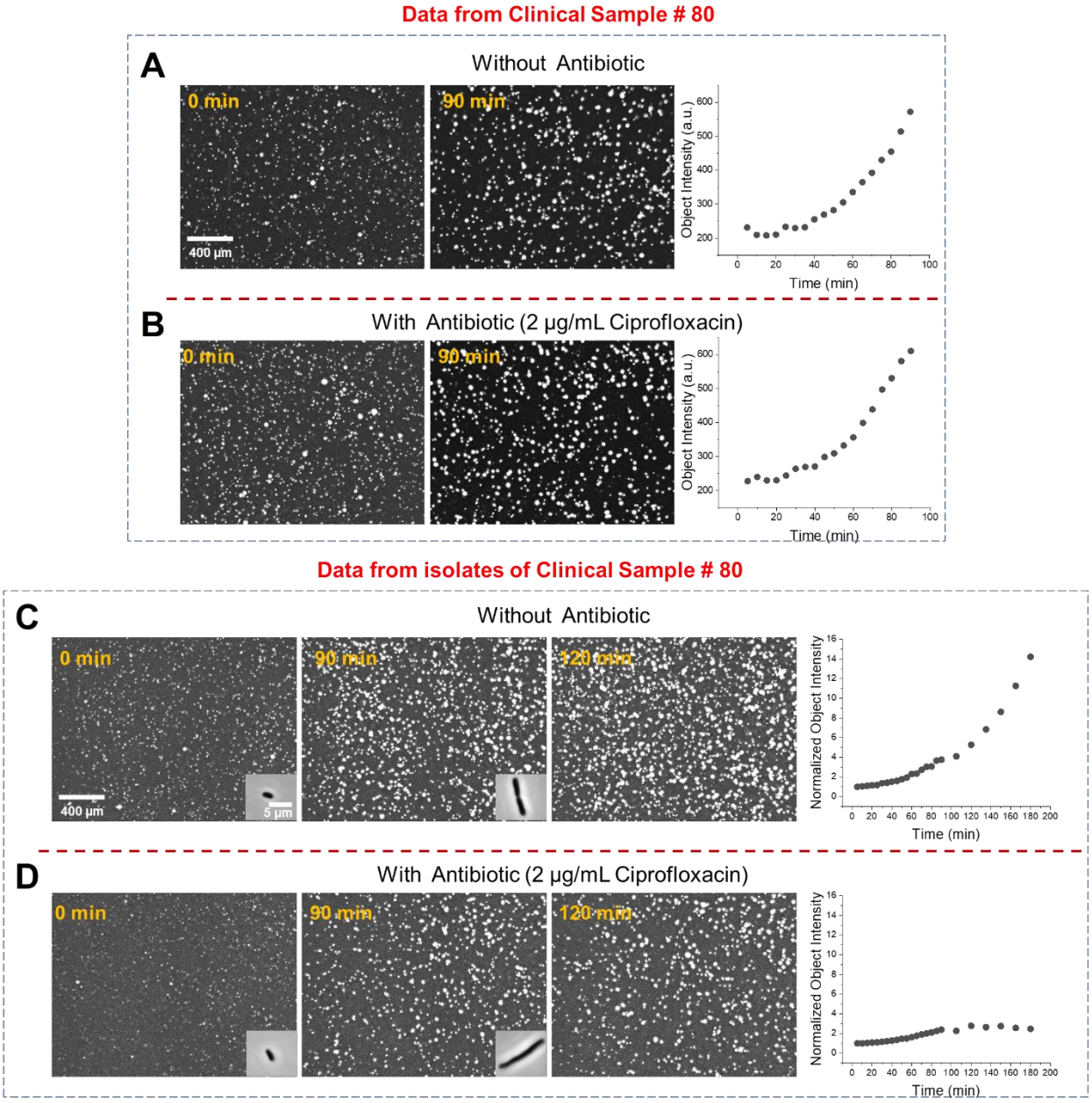


**Figure S10. Background removed LVSi images at different time points and object intensity curves for clinical sample # 80 (A, B) and cryogenically-preserved clinical sample #80 (C, D) without (A, C) and with antibiotics (B, D).** The insets in C and D are the corresponding high magnification (80×) cell image for morphology validation.

### S13. MIC determination for OSID-AST

The minimum inhibitory concentration (MIC) of ciprofloxacin and nitrofurantoin were determined for OSID-AST with 90 min exposure of different concentrations of the antibiotic. The normalized object

intensity ($I_{90}/I_0$) of *E. coli* cells with 0 μg/mL, 0.5 μg/mL, 1 μg/mL, 2 μg/mL, 4 μg/mL, and 8 μg/mL ciprofloxacin were calculated for the inhibition curve plot (Supporting Information Figure S11A), while the nitrofurantoin concentrations tested were 0 μg/mL, 4 μg/mL, 8 μg/mL, 16 μg/mL, 32 μg/mL, 64 μg/mL and 128 μg/mL (Supporting Information Figure S11B). The MIC value is defined as no growth in object intensity where normalized object intensity equals 1 (dashed lines in Figure S11). The MIC value is determined to be 1 μg/mL for ciprofloxacin and 4 μg/mL for nitrofurantoin.

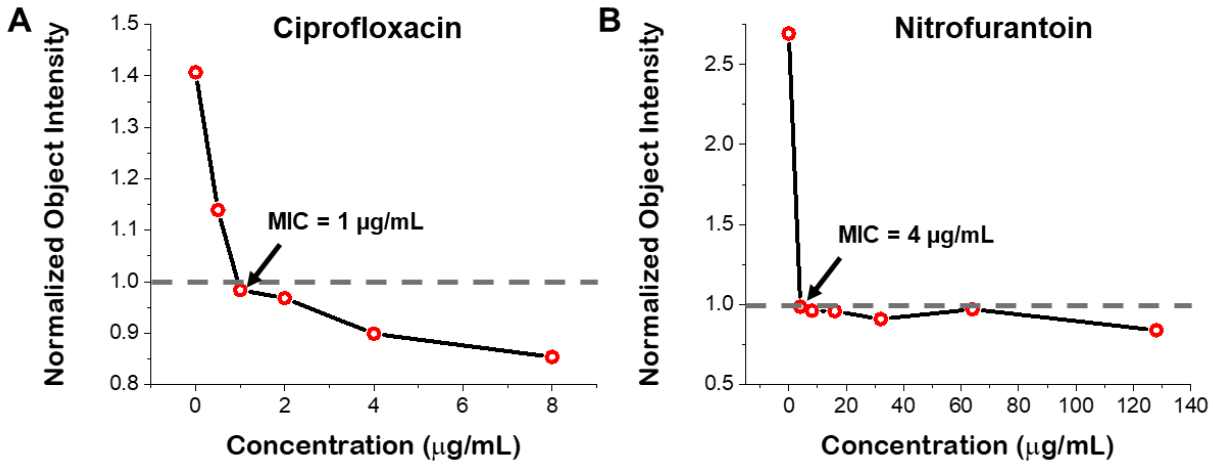


**Figure S11. The inhibition curves of OSID-AST after 90 min exposure of ciprofloxacin (A) and nitrofurantoin (B).** The MIC value is determined by the minimum concentration that no growth induced object intensity increase (dashed lines) detected by OSID-AST.